Dynamic spreading characteristics of droplet impinging soybean leaves

He Li, Xiaoxiao Niu, Li Ding*, Ali Shahid Tahir, Changle Guo, Jiajun Chai, Kaifei Zhang, Shangshang Cheng, Yiqiu Zhao, Yahui Zhang, Yigao Xu, Zengqiang Shang

(*College of Mechanical & Electrical Engineering, Henan Agricultural University, Zhengzhou 450002, China*)

Abstract: The study on the deposition efficiency of pesticide droplets on soybean leaves can provide the basis for reducing pesticide quantity and increasing pesticide efficiency during the application of soybean plant protection machinery. The movement behavior of droplet impinges on the plant leaf surface is affected by many factors, among which the most important and the easiest to adjust are spray droplet size and impingement velocity. By changing the droplet size and impact velocity and using Fluent simulation software, the pesticide droplet hitting the soybean leaf surface was simulated and a test platform was established to verify the simulation results. The conclusions are as follows: The longitudinal roughness of soybean leaves is higher than the transverse roughness, the longitudinal pressure of soybean leaves is higher than the transverse pressure during the impact process, and the velocity of droplet spreading along the longitudinal is lower than that of spreading along the transverse; although soybean leaf surface has high adhesion, droplet losses still exist when droplet impact velocity is relatively high. The maximum spreading diameter of the droplet increases first and then decreases with the increase of impact velocity. At the same time, the maximum spreading diameter of droplet increases with the increase of particle size. The droplet deposition was best at 1.34 m/s impact velocity and 985 μm particle size. This conclusion can provide optimal operation parameters for soybean plant protection operation which can be used to guide soybean plant protection operation, improve control effect, reduce quantity and increase efficiency.

Keywords: soybean, deposition efficiency, Fluent, droplet impact, spreading features, dynamic

DOI: 10.25165/j.ijabe.20211403.6274

Citation: Li H, Niu X X, Ding L, Tahir A S, Guo C L, Chai J J, et al. Dynamic spreading characteristics of droplet impinging soybean leaves. Int J Agric & Biol Eng, 2021; 14(3): 32–45.

1 Introduction

The effective use of pesticides can influence control effect, reduce cost, protect the ecological environment and improve crop quality. The movement of droplets against plant leaves will decide whether pesticides can be effectively deposited on the surface of plant leaves during plant protection application. So, in order to improve pesticide utilization rate, it is very important to study the kinematics and dynamics of droplets impinging on the surface[1]. Droplet impingement on the plant leaf surface is affected by many factors, such as physical and chemical parameters like the surface tension of droplet, viscosity, density, particle size, tilt angle, the speed at which the droplet impinges on the blade surface; biological properties like the roughness of the blade surface, contact angle, wetting ability; environmental factors like site temperature and humidity, wind speed. Among them, the most important and the easiest to adjust are the spray droplet size and velocity[2,3]. In addition, the spreading behavior of droplet impinging on blade surface is closely related to fluid mechanics and surface physics, etc.[4,5]

The microscopic appearance of droplets impinging on a surface has always been a research hotspot. Song et al.[6] used "the seesaw effect" to show the basic physics of orientation bounce after droplets hit a heterogeneous interface. Boukhalfa et al.[7] found the chemical composition of the solution played a decisive role in the droplet adhesion to the leaf surface, through high-speed imaging and fluorescence detection to study the drops that hit the barley leaves. Nairn et al.[8] found the basic principle of leaf blade with hairy structure, which will help improve its spray effectiveness; Maher et al.[9] studied drop impact and coupling dynamic of blade surface deposition formation using high-speed imaging technology, and developed a physical model to predict the energy dissipation of droplets, it provided an important theoretical basis for the effective improvement of pesticide utilization. Liang[10] recorded droplets hitting solid surfaces at different angles of contact at the same speed by high-speed imaging technology. Bi et al.[11] used high speed imaging technology to study the influence of droplet motion pattern during impact by different droplet impact parameters, and found that the adhesion played a major role in the spreading process of droplet, the surface tension played an important role in the withdrawal process of droplet, and

Received date: 2020-11-19 **Accepted date:** 2021-04-08

Biographies: He Li, PhD, Professor, research interests: design and control of agricultural equipment, Email: chungbuk@163.com; **Xiaoxiao Niu**, MS candidate, research interests: agricultural equipment and control system, Email: 15637863325@163.com; **Ali Shahid Tahir**, PhD, research interests: agricultural equipment and control system, Email: 3508313416@qq.com; **Changle Guo**, MS, research interests: agricultural equipment and control system, Email: 1943235984@qq.com; **Jiajun Chai**, MS candidate, research interests: agricultural equipment and control system, Email: 2118728973@qq.com; **Kaifei Zhang**, PhD, Professor, research interests: agricultural equipment and control system, Email: zhangkaifei1220@163.com; **Shangshang Cheng**, MS candidate, research interests: agricultural equipment and control system, Email: 1228274702@qq.com; **Yiqiu Zhao**, Master, research interests: agricultural equipment and control system, Email: 670501084@qq.com; **Yahui Zhang**, MS candidate, research interests: agricultural equipment and control system, Email: 2013454114@qq.com; **Yigao Xu**, MS candidate, research interests: agricultural equipment and control system, Email: 1003288622@qq.com; **Zengqiang Shang**, MS candidate, research interests: agricultural equipment and control system, Email: 17337309582@163.com.

***Corresponding author: Li Ding**, PhD, Lecturer, research interests: agricultural equipment and control system. College of Mechanical & Electrical Engineering, Henan Agricultural University, Zhengzhou 450002, China. Tel: +86-18310047056, Email: 604295294@qq.com.

the oscillation process of droplet was determined by both. Xie et al.[12] studied the spreading process of the droplet (high-efficiency cypermethrin emulsion) hitting the leaf surface of the wolfberry, the results showed that the final spreading coefficient of the droplet was affected by droplet size, the impact speed, angle of blade tilt, and so on. Influence factors of droplet impingement on blade surface were as follows: angle of blade tilt, the structure of the blade surface, droplet size, which was studied by Wang[13] who used an orthogonal experimental design.

In recent years, CFD computational fluid Dynamics simulation analysis technique, as an aid, has been widely used in detection research by most scholars, in order to simulate the physical behavior of droplets when they hit a solid surface[14-21]. For example, Liang et al.[15] studied how the physical behavior of droplets changed when they hit planes with different contact angles, through VOF to simulate the whole physical behavior process of droplet; Xie et al.[12] carried out experimental research and simulation analysis on the leaf spreading characteristics of lyceum barbarum impacted by droplet. The dynamic behavior of droplet impacting interface has become a hot research object, the number of papers published is increasing. However, there are still few reports on droplet impact on the leaf surface of soybean plant. Unlike the droplet hitting the plane, there are many conical hairy structures on the leaf surface of soybean that has irregularly distributed curved meridional structure and strong adhesion. In this paper, summer soybean leaves in the Huang-Huai-Hai area were selected as experimental materials to study the spreading characteristics of droplet on the surface. In the simulation software (Fluent), the droplet impingement on soybean leaf surface was simulated and analyzed by inputting the blade properties into the wall properties and setting different impact velocities and particle sizes. Then, the simulation results are verified by high speed imaging technology. Finally, the spreading characteristics of the droplet impacting the soybean leaf surface were obtained. It provides the basic theoretical basis for improving the deposition efficiency of droplet spreading on the blade surface, reducing the amount and increasing the efficiency.

2 Analysis of droplet impingement process

The droplets spread out as they hit a solid surface, this process causes the kinetic energy to dissipate as it overcomes the viscous forces to form new droplet shapes. The surface tension and capillary force of the droplet prevent it from spreading on the solid surface, which causes droplet withdrawal that can make the kinetic energy of the droplet increase. During the withdrawal if the inertia force of the droplet is sufficient to cause the droplet to rise from the solid surface, the droplet will rebound or partially rebound which will sputter out small droplets; otherwise, the droplets begin to spread out over the solid surface again. Then, it will spread out and vibrate on the solid surface. Finally, it will be deposited on the surface when energy dissipation reaches equilibrium[22,23]. So the process of impact can be divided into pre-impact, impact spread to the maximum stage, droplet withdrawal stage, the drop spread to the withdrawal stage causes the drop to rebound, sputtering, sedimentary, tumble, and so on (Figure 1).

2.1 Stage before the droplet hits the surface

The droplet is not affected by the solid surface material and wettability before the droplet hits the surface. The drop remains spherical under the influence of surface tension. E_{K0} represents the kinetic energy of the droplets before impact[24], E_{S0} represents the initial surface energy. The kinetic energy of the droplets and the initial surface energy are shown below separately:

$$E_{K0}=\left(\frac{1}{2}\rho U_0^2\right)\left(\frac{1}{6}\pi D_0^3\right) \tag{1}$$

$$E_{S0}=\sigma_{LG}\pi D_0^2 \tag{2}$$

where, U_0 is the initial velocity of the droplet before impact, m/s; D_0 is the diameter of the droplet, mm; ρ is the droplet density, g/cm^3; σ_{LG} is the surface tension between gas and droplet, mN/m.

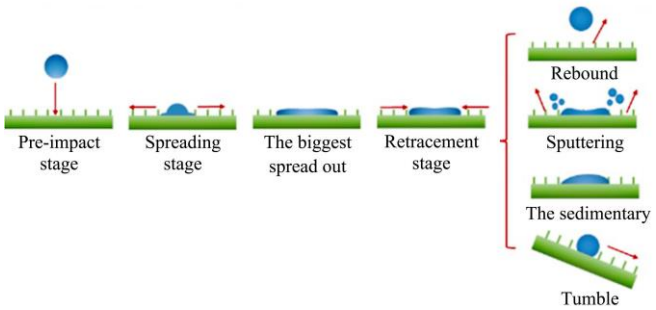

Figure 1 Droplet impact rough surface simulation

2.2 Droplet spreading stage

Under the action of inertia force and surface adhesion force, the droplet impinges on the surface and begins to spread into the liquid film. The droplet reaches its maximum spreading diameter at the end of the spreading stage. Dong et al.[25] analyzed the process in terms of the conservation of energy. They found that kinetic energy was converted to internal energy as the droplets spread out.

$$E_{K1}=0 \tag{3}$$

At this time, the surface energy can be obtained by using Equation (4).

$$E_{S1}=\frac{1}{4}\pi\sigma_{LG}D_{\max}^2(1-\cos\theta) \tag{4}$$

where, E_{K1} is the kinetic energy, J; E_{S1} is the surface energy, J; $D_{\max}$ is the maximum spreading diameter of the droplet after it hits the surface, mm; θ is the contact angle, (°).

During the spreading process, the liquid droplets change from the solid-gas interface before the impact to the solid-liquid interface after the impact. Therefore, the surface energy changes as below,

$$E_P=\frac{1}{4}\pi D_{\max}^2(\sigma_{SL}-\sigma_{SG}) \tag{5}$$

where, E_P is the surface energy after impact, J; σ_{SL} is surface tension between solid and droplet, mN/m; σ_{SG} is surface tension between solid and gas, mN/m.

When the droplet overcomes the viscous force and other resistance during the impact process, it forms a new droplet shape and energy dissipates. The viscous dissipation equations are as follows[26]:

$$W=\int_0^{t_0}\int_V \varnothing dVdt\approx\varnothing Vt_c \tag{6}$$

$$\varnothing=\mu\left(\frac{\partial U_i}{\partial x_j}+\frac{\partial U_j}{\partial x_i}\right)\frac{\partial U_i}{\partial x_j}\approx\mu\left(\frac{U_0}{h}\right)^2 \tag{7}$$

$$t_c\approx\frac{D_0}{U_0} \tag{8}$$

where, t_c is the characteristic time of viscous dissipation, ms; h is the thickness of the liquid film, mm; μ is the viscosity coefficient, MPa s.

The integral volume can be approximately expressed as the following equation:

$$V \approx \frac{1}{4}\pi D_{\max}^2 h \tag{9}$$

The thickness of the liquid film is as shown below, obtained by volume conservation.

$$h = \frac{2}{3}\frac{D_0^3}{D_{\max}^2} \tag{10}$$

Put the above parameters into the energy conservation equation to obtain the following equation:

$$W \approx \frac{1}{4}\pi\mu\left(\frac{D_0}{h}\right)D_0 D_{\max}^2 \tag{11}$$

Young's equation is shown below:

$$\sigma_{lv}\cos\theta = \sigma_{sv} - \sigma_{ls} \tag{12}$$

The energy conservation equation before and after impact is shown as

$$E_{K0} + E_{S0} = E_{K1} + E_{S1} + W \tag{13}$$

From Equations (8), (9), and (11), the following equation can be obtained:

$$\frac{2}{3}\beta_{\max}^4 + (1-\cos\theta)\beta_{\max}^4 - \left(\frac{1}{3}We + 4\right) \approx 0 \tag{14}$$

$$We = \frac{\rho U^2 D_0}{\sigma} \tag{15}$$

$$Re = \frac{\rho U D_0}{\mu} \tag{16}$$

where, U is the velocity of droplet impact, m/s; σ is the surface tension, mN/m; $\beta_{\max}$ is the maximum spreading coefficient of droplet.

When Weber number We<<Reynolds number Re, $\beta_{\max}$ can be approximately expressed as the following equation:

$$\beta_{\max} = \left[\frac{1}{3}(We + 4 \diagup (1-\cos\theta)\right]^{1/2} \tag{17}$$

2.3 Droplet withdrawal stage

After the liquid hits the solid surface and spreads out to the maximum extent, the droplet retracts due to surface tension and capillary force. At this time, the kinetic energy of the droplet increased, and it appeared interaction force between the surface droplets and soybean leaves. Droplets begin to deposit, sputter, or bounce off, and there are potential energy and surface energy coming out in the droplets[24], which are shown as follows equations:

$$E_{K2} = \pi\rho g\int_0^{h_m} x^2 y dy \tag{18}$$

$$E_{S2} = 2\pi\gamma_{LV}\int_0^{h_m} x\sqrt{1+[f'(y)]^2}dy - \sigma_{LV}\pi x_0^2\cos\theta \tag{19}$$

$$E_2 = E_{K2} + E_{S2} \tag{20}$$

2.4 Droplet rebound, sputtering and deposition stage

From the pre-crash stage to the retracement stage, the amount of energy will show different impact behavior. If the impact kinetic energy is much greater than the surface energy of the droplet, the droplet will appear rebound phenomenon or sputter out small droplet; if the impact kinetic energy is not enough to overcome the potential energy, the droplet will not leave the blade surface, but spread out and vibrate, so as to achieve an equilibrium of energy dissipation and deposit on the blade surface[24].

The surface energy of the droplet as it bounces is shown as below,

$$E_{S3} = \pi D_0^2\sigma_{LG} \tag{21}$$

At this time, the droplet potential energy is far less than the surface energy, so the total energy of the droplet is shown below,

$$E_3 \approx E_{S3} \tag{22}$$

Since the total energy of the droplet (kinetic energy and surface energy) is conserved, the equation is as follows.

$$\frac{1}{2}\rho h_{sh} L U_{sh}^3 + 2LU_{sh}\sigma = \frac{1}{2}\frac{\pi}{4}\rho d_j^2 U_j^3 + \pi d_j U_j \sigma \tag{23}$$

where, h_{sh} is the height of the droplets, mm; L is the maximum spreading diameter of droplets, mm; U_j is the sputtering impact rate of droplets, m/s; d_j is the sputtering droplet diameter, mm.

In this study, the surface wetting characteristics were analyzed, and the dimensionless number, fluid mechanics, surface dynamics and energy conservation principles were adopted to provide a theoretical basis for the study on the surface spreading characteristics of soybean leaves impacted by liquid drops according to the previous basic theories on the surface process of liquid drops.

3 Simulation analysis of droplet impinging soybean leaf surface

3.1 Calculation model

Couple Level Set+Volume of Fluid (CLSVOF) is a tracking method that is used in multiphase flow in numerical simulation. CLSVOF combines the advantages of both the VOF and Level Set. This makes it not only have the property of energy conservation, but also be able to accurately calculate the curvature and the physical quantities related to the curvature, and also be able to smooth the physical quantities of abrupt change at the phase interface. Figure 2 shows the computational flow of the phase interface tracking process using the CLSVOF method.

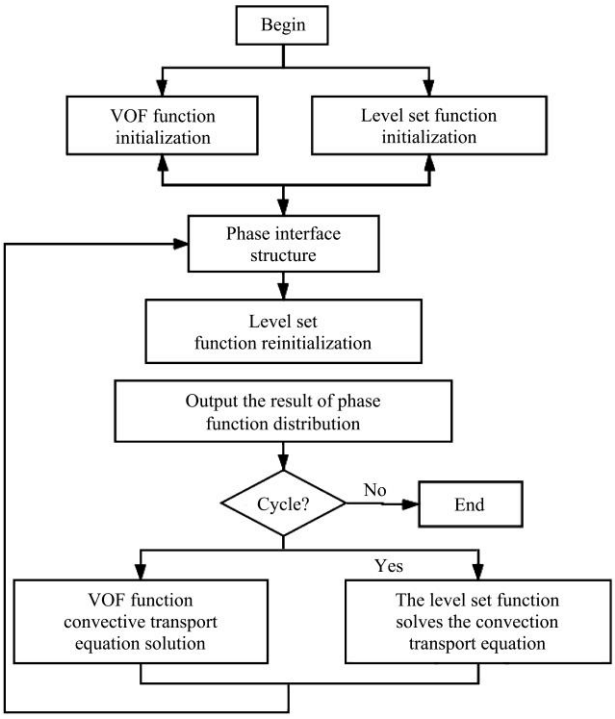

Figure 2 CLSVOF tracking interface flow chart

3.2 Determination of soybean leaf surface characteristics

Soybean leaf surface has a very complicated surface structure, and there are also protective wax and fluff on the surface, which affect the surface roughness of soybean leaf surface, and thus affect the interface deposition mechanism after droplets hit the leaf surface. In this study, an atomic force microscope (AFM) was used to observe the surface of soybean leaves in detail, and to measure the surface roughness and waxy properties of soybean leaves. Measured under the atomic force microscope, soybean

leaf characteristics have different surface roughness in the horizontal and vertical directions. The horizontal length of the leaf surface is l_1=4.82 mm, and the surface roughness is Ra_1= 10.9 nm; the vertical length is l_2=12.05 mm, and the surface roughness Ra_2=41.5 nm.

The OCA25 video optical contact angle measuring instrument was used to measure the contact angle of soybean leaves as shown in Figure 3, and the data of the contact angle of the droplets on the surface of soybean leaves are shown in Table 1. Among them, the average contact angle of the soybean leaf surface is 128.76°, and the static contact angle of the soybean leaf is relatively stable, and the hydrophobicity is significant.

Note: A, B and C are three droplets at different positions of the blade, and the changes of contact angle at different positions is not significant.

Figure 3 Pictures of measuring the contact angle

Table 1 Measurement values of soybean leaf contact angle

No.	Left contact angle	Right contact angle	Mean contact angle
1	127.32°	125.92°	126.62°
2	128.51°	128.40°	128.45°
3	131.20°	130.37°	130.78°
4	126.53°	126.05°	126.29°
5	131.82°	131.31°	131.56°
6	128.92°	128.48°	128.87°
Average	129.05°	128.48°	128.76°

When the soybean is used for drug control, the 5% highly effective cyhalothrin microemulsion 1000 times liquid is generally used[26], and the surface tension of the pesticide is 7.308×10^{-2} N/m measured by the maximum bubble method; NDJ-8S digital display viscosity. The viscosity coefficient of pesticide measured by the meter is 2.98 MPa s

3.3 Establishment of a model of pesticide droplet impacting soybean leaf surface

The length of the leaf surface is 12.05 mm and the width is 4.82 mm. Based on the soybean leaf surface parameters, a two-dimensional leaf surface model was established in Fluent. The meshing software ICEM-CFD was used to establish horizontal and vertical calculation domains on the leaf, using the framework-based modeling approach, as shown in Figure 4. The geometric shape in the calculation model is a circle with a diameter of D= 900 μm, which is the initial position of the pesticide drop; the height of the drop is H = 500 μm; the wall is the bottom boundary

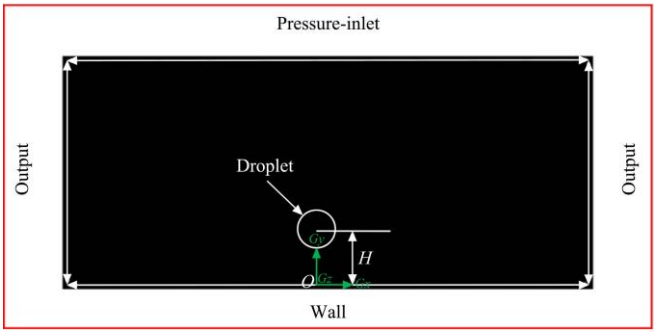

Figure 4 Calculation model and boundary conditions of droplet impacting soybean leaf surface

condition in the calculation model, and represents the soybean leaf surface. And all parameters of soybean leaf surface can be set in boundary conditions; the left and right sides of the boundary are set as pressure outlets. When the initial velocity of the pesticide droplet impact is large enough, it may move from the pressure outlet boundary to the outside of the calculation domain when spreading on the surface of soybean leaves; the boundary condition of the top side is set as the pressure inlet.

3.4 Analysis and calculation of the deposition results of pesticide droplets impacting soybean leaves

According to the measured value of the soybean leaf contact angle obtained in Table 1, the contact angle between the droplet and the soybean leaf surface in the numerical simulation calculation process is 129°, which does not change with the time step of impact; the target angle is 90°, which means vertical impact. The droplet size used for soybean application is 900-1000 μm, and the velocity of the droplet impacting the leaf surface is 1.0-1.5 m/s[27]. On the one hand, let the droplet size be 900 μm, select the impact velocity 1.03 m/s, 1.34 m/s, 1.55 m/s, respectively, and analyze the influence of different impact velocities on the spreading characteristics of droplets; On the other hand, let the impact velocity be 1.34 m/s, select the droplet size of 900 μm, 925 μm, 960 μm, 985 μm respectively, and analyze the influence of different particle size on the droplet spreading characteristics. In this study, the influence of different impact velocity and droplet size on droplet spreading characteristics was analyzed from the liquid phase, surface wettability, pressure and velocity distribution of the transverse and longitudinal surfaces of the blades in the post-processing of numerical simulation calculation results, so as to provide new ideas and methods for improving pesticide utilization.

3.4.1 Liquid phase

Figure 5 shows the liquid phase distribution diagram, at each moment after the droplet with three different impact velocities vertically hits the soybean leaf in the transverse direction of the leaf surface, when the droplet diameter is 900 μm and the impact height is 500 μm. Obviously, the dynamic behavior evolution of a single droplet under different impact speeds after impacting the leaf surface also has similar changes in the corresponding characteristic time. The dynamic behavior changes in these liquid phases include the following three stages: spreading, shrinking and deposition. As shown in Figure 5a, when the impact velocity is 1.03 m/s, at t=1 ms, the droplet begins to spread, and it stays in the spreading state until t=2 ms and reaches the maximum spreading length when t=3.5 ms; at t=6 ms, the droplet begins to shrink; then, at t=8 ms, it shrinks into the main droplet, and finally deposits at t=12 ms.

As shown in Figure 5b, when the impact velocity is 1.34m/s, at t=1 ms, the droplet begins to spread, and it stays in the spreading state until t=2 ms and reaches the maximum spreading length when t=3 ms. The droplet begins to shrink until t=6 ms; then, it shrinks into a main droplet at t=8 ms, and finally deposits at t=12 ms.

As shown in Figure 5c, when the impact velocity is 1.55 m/s, at t=1 ms, the droplet begins to spread, and the droplet hits the leaf surface to sputter many small droplets, the main droplet remains to spread until t=2 ms; when t=3.5 ms, the two sides of the spreading droplet exceed the boundary of the leaf surface, and the volume of the liquid phase decreases, at this time, the droplet reaches the maximum spreading length. The droplet begins to shrink until t=6 ms; then, at t=8 ms, it shrinks into two droplets, and two droplets finally deposit at t=12 ms.

The difference of the dynamic evolution of the above-mentioned droplets on the blade surface over time is mainly affected by different impact speeds. The maximum spreading diameters of droplets first increase and then decrease with the increase of the impact speed. At the impact speed of 1.34 m/s, the maximum spreading diameter of the droplet reaches the maximum.

Figure 6 shows the liquid phase diagram at the time of the maximum spreading diameter of droplets with different particle sizes along the transverse direction when the impact velocity is 1.34 m/s. It can be seen from Figure 6 that when the impact velocity is 1.34 m/s, the maximum spreading diameter of the 900 μm droplet is 2069 μm and the maximum spreading coefficient is 2.30; the maximum spreading diameter of the 925 μm droplet is 2150 μm, and the maximum spreading coefficient is 2.32; The maximum spreading diameter of the 960 μm droplet is 2258 μm, and the maximum spreading coefficient is 2.35; The maximum spreading diameter of the 985 μm droplet is 2483 μm, and the maximum spreading coefficient is 2.52. Therefore, when the droplet size is 985 μm, it has a better deposition effect than other selected size droplets.

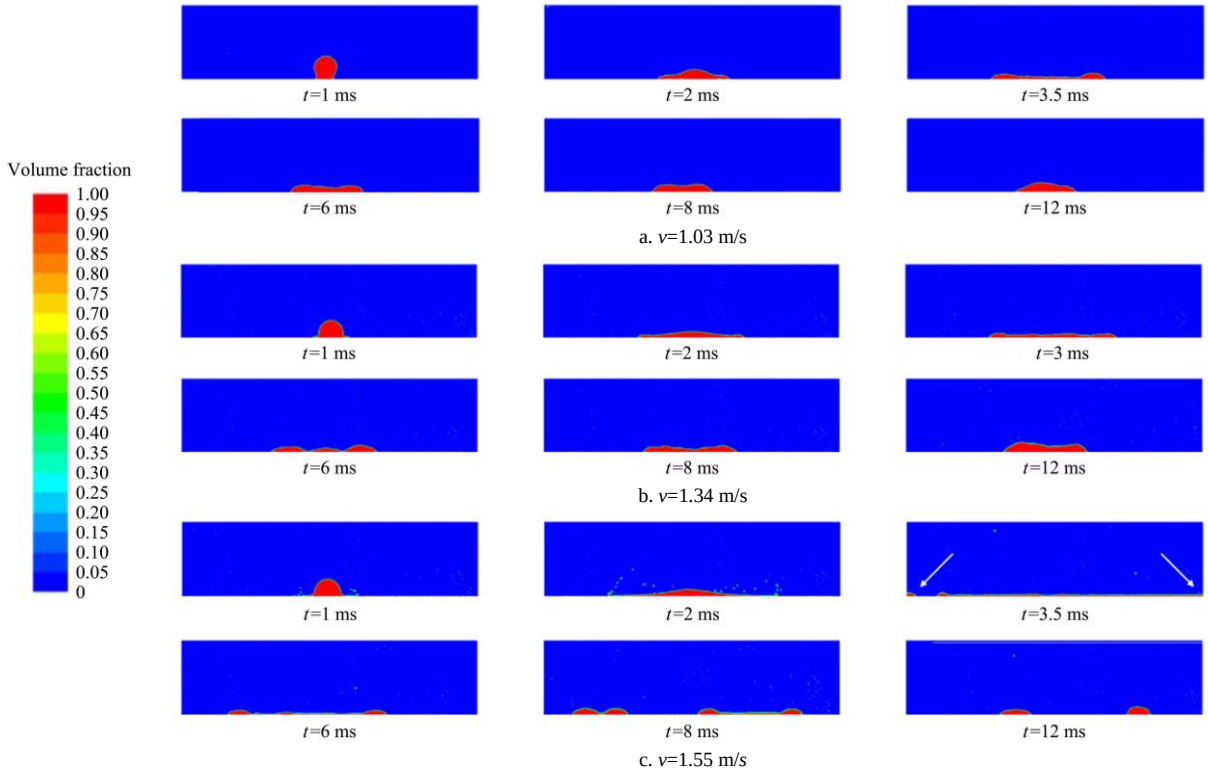

Figure 5 Variation diagram of spreading liquid phase with time under three impact velocities as droplet impinged on soybean leaf surface (transverse)

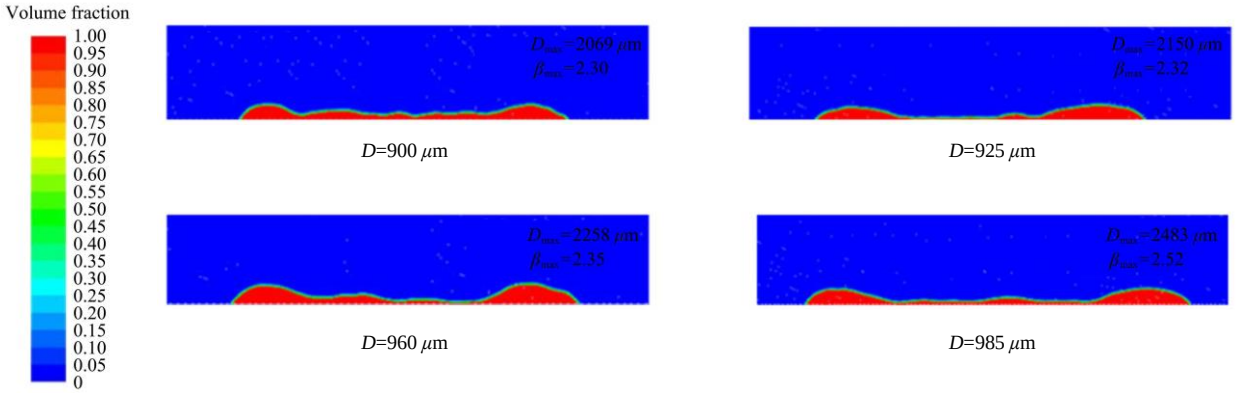

Note: Impact velocity is 1.34 m/s. D represents the droplet diameter. D_{max} is Maximum spreading diameter. β_{max} is Maximum spreading coefficient.

Figure 6 Liquid phase diagram at the moment of maximum spreading diameter of droplets under different particle sizes (transverse)

Figure 7 shows the liquid phase distribution diagram, at each moment after the droplet with three different impact velocities vertically hits the soybean leaf in the longitudinal direction of the leaf surface, when the droplet diameter is 900 μm and the impact height is 500 μm. As observed in Figure 7, during the spreading process of the three droplets after impact, the dynamic evolution of the droplet shape has also undergone similar changes: spreading, shrinking and deposition. However, in the corresponding characteristic time, there are obvious differences between the transverse and longitudinal directions: 1) In the spreading stage, when the impact velocity is 1.34 m/s, the characteristic time of the droplet in the transverse direction is 0.5 ms faster than that in the longitudinal direction. The former is 3.0 ms and the latter is 3.5 ms. When the impact velocity is 1.03 m/s and 1.55 m/s, the characteristic time of the droplet along the longitudinal direction is 3.0 ms, which is 0.5 ms faster than the characteristic time along the transverse direction; 2) In the splitting stage, all droplets in the transverse direction split into the first droplet from the right side of

the liquid film, while in the longitudinal direction, all droplets with different impact velocities split into the first droplet from the left end of the liquid film.

Comparing Figure 5 with Figure 7, it can be known that the droplets along the longitudinal direction are generally easier to split and break. In order to analyze the phenomenon of breakage after the droplets hit the soybean leaf surface, the velocity distribution vector diagram after the droplet hit the soybean leaf surface was obtained (Figure 8). Figure 8a is a vector diagram of the velocity distribution of the droplets before they hit the soybean leaf surface. The yellow curve is the gas-liquid interface of the droplets. The movement of the droplets after they hit the wall is basically symmetrical. It can be seen from the figure that before the droplet hits the leaf surface and breaks, the middle part of the droplet is in a state of adhesion. The liquid velocity on both sides of the middle adhesive part moves away from each other, and the adhesive part is about to separate. At the same time, due to the resistance of the leaf surface below the adhesion part, the flow velocity under the adhesion part is lower than the upper flow velocity. The difference in the upper and lower flow velocity formed by the resistance of the leaf surface promotes the separation of the liquid of the middle adhesive part. The greater the roughness of the leaf surface, the more obvious the difference between the upper and lower flow velocity of the liquid part to be broken. Therefore, under the combined action of the internal movement of the droplet and the leaf resistance, the middle part of the droplet gradually becomes thinner. Then there was a break in the middle of the droplet, as shown in Figure 8b, and the phenomenon of shrinkage and fragmentation occurs. After the droplet is broken, the broken place gradually moves to the left and right sides under the action of the surrounding gas vortex and the internal momentum of the droplet, so that the two parts of the broken liquid will be in a retracted state until they become stable. Research on the breaking phenomenon of droplets after impacting the leaf surface, it is found that the greater the roughness of the leaf surface, the easier the droplets are broken after impacting the leaf surface.

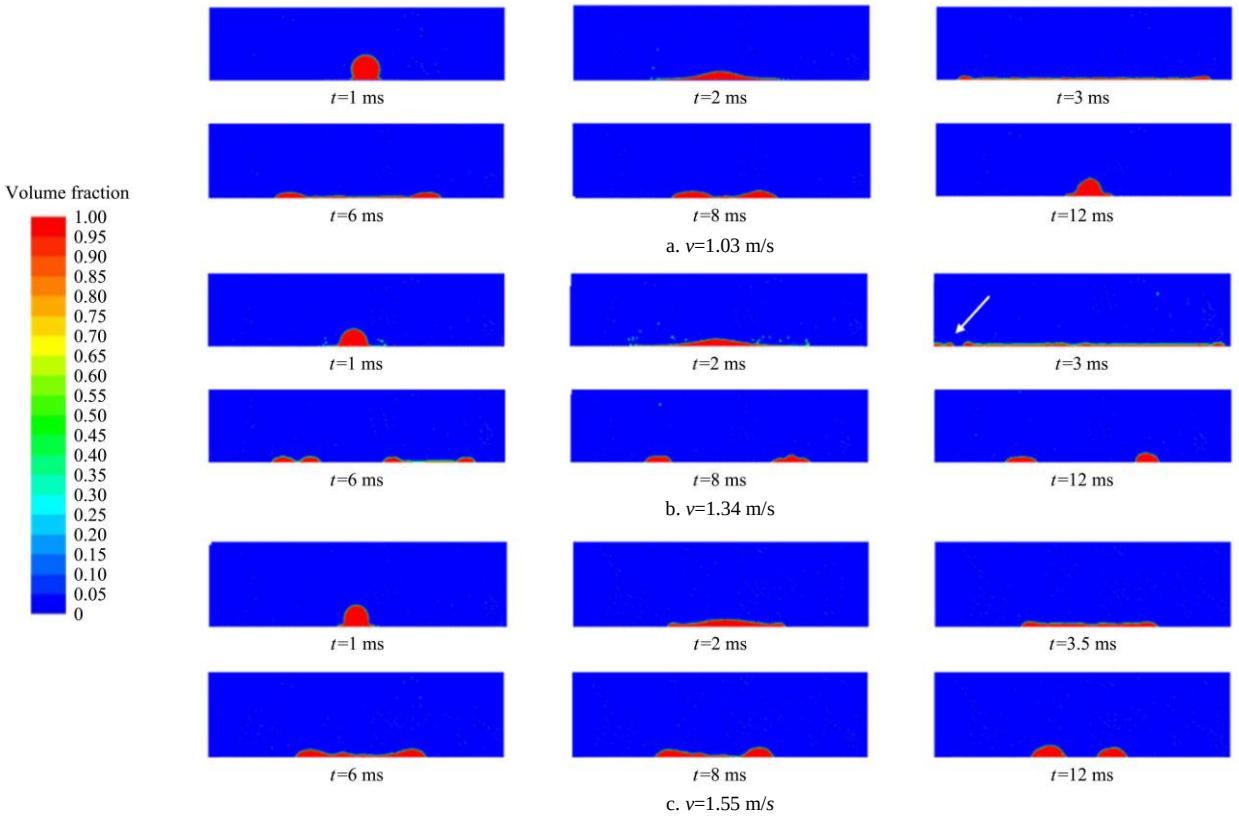

Figure 7 Changes of spreading liquid phase with time when droplet impinged on soybean leaf surface under three impacting velocities (longitudinal)

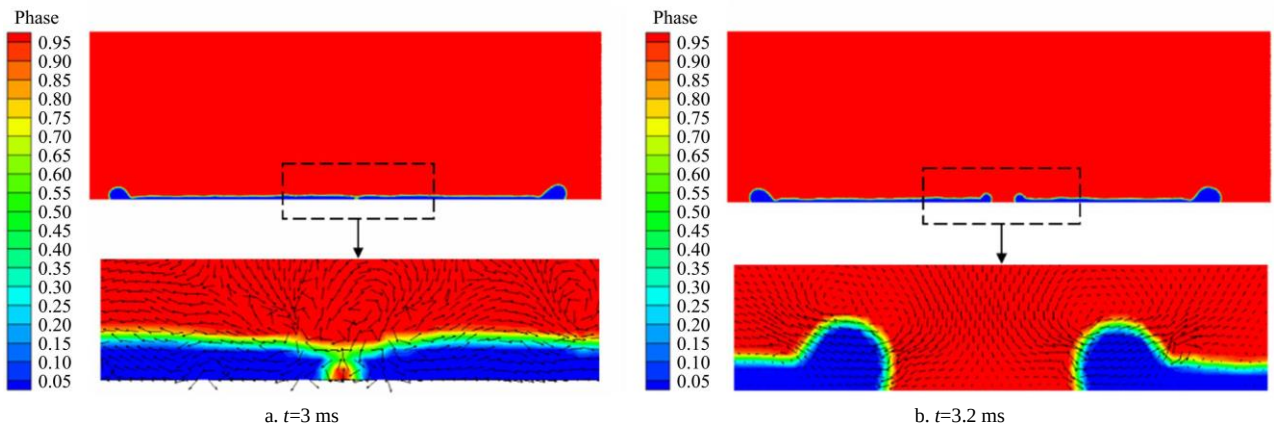

a. t=3 ms b. t=3.2 ms

Figure 8 Velocity vector distribution of droplet impacting soybean leaf surface

When the impact velocity is 1.34 m/s, the liquid phase diagram at the time of the maximum spreading diameter of the droplets under different particle sizes is shown in Figure 9. In general, there is no difference in the liquid phase diagram of droplets of different sizes along with the transverse and longitudinal directions when they hit the leaf surface. The order of spreading ratio of different size droplets is 985 μm > 960 μm > 925 μm > 900 μm. When the droplet size is 985 μm, it has a better deposition effect than other droplets.

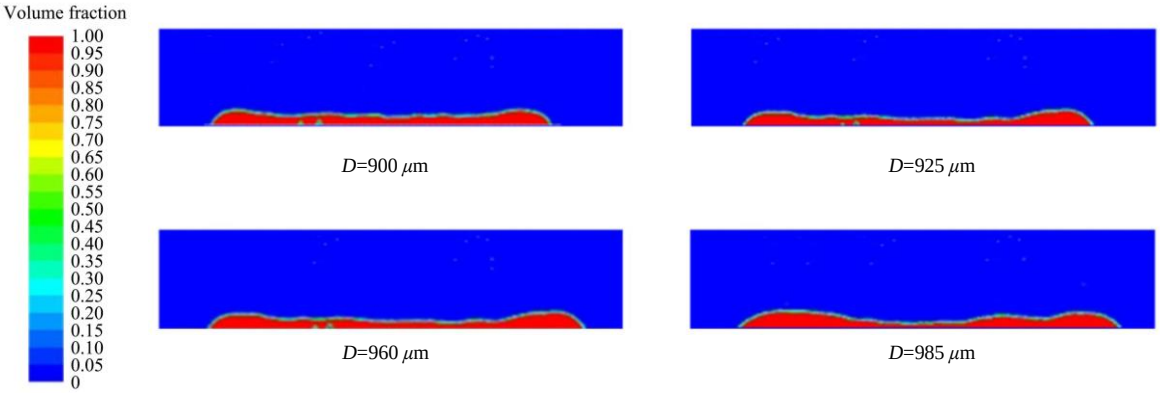

Note: Impact velocity is 1.34 m/s. *D* represents the droplet diameter.

Figure 9 Liquid phase diagram at the moment of maximum spreading diameter of droplet under different particle sizes (longitudinal)

3.4.2 Pressure

Figure 10 shows the pressure changes of three droplets with different impact velocities after vertical impact on the soybean leaf. The pressure here represents the pressure of the droplet from impact to deposit on the soybean leaf surface, as shown in Figure 10. For all droplets, the droplet did not impact the wall surface before t=0.9 ms at first, and the pressure was zero; Then, at t= 1.1 ms, the droplet collided with the wall surface, and the pressure increased to the maximum value. At t=2.2 ms, the droplet was deposited on the blade surface, and the pressure dropped to zero again. When the impact velocity is 1.55 m/s, the pressure value is the highest in the transverse or longitudinal direction, about 0.184/0.230 MPa, followed by 1.34 m/s and 1.03 m/s. When the impact velocity was 1.34 m/s and 1.03 m/s, the maximum pressure value of droplet was 0.138/0.138 MPa and 0.123/0.126 MPa, respectively.

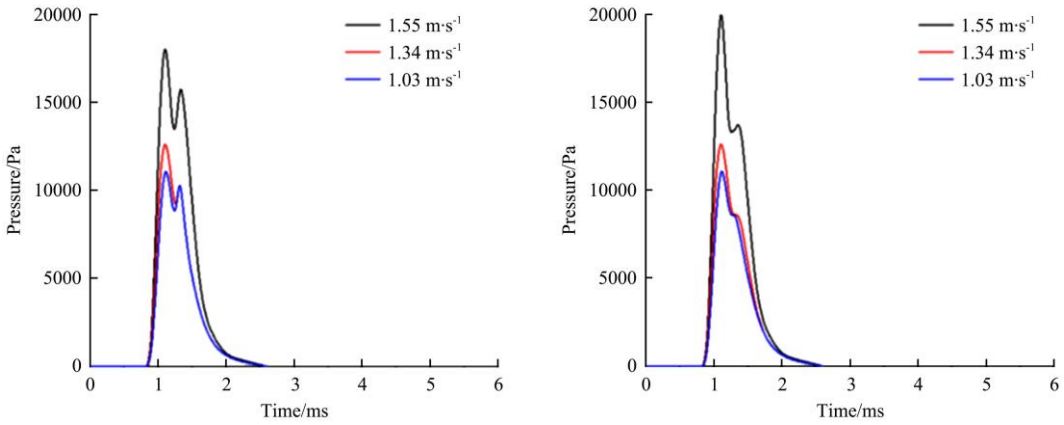

Figure 10 Changes of pressure on soybean leaf surface impacted by droplet with time under three different impact velocities

For different impact velocities, it can be seen that the pressure values along the transverse direction are always lower than that along the longitudinal direction. This can be explained that the pressure caused by droplet impact is closely related to the roughness of the blade surface. In detail, the pressure acting on the soybean leaf surface during the post-impact oscillatory spreading process is determined by two key factors: weight and deformation. Since the droplet diameter D = 900 μm, in the numerical simulation, the effect of gravity is negligible. Therefore, the pressure caused by droplet impact deformation plays a dominant role. The relevant equation is as follows:

$$\Delta P_2' = \frac{2\sigma}{R} \quad (24)$$

where, σ is surface tension, mN/m; R is the droplet spreading radius on soybean leaf, mm.

In the oscillation spreading process after impact, the change of droplet radius is related to the surface roughness. It can be seen from Figure 11 that the larger the surface roughness is, the smaller the spreading radius of droplet is on the surface of soybean; and according to Equation (24), the smaller the spreading radius is, the greater the pressure is. In summary, the pressure increases with the increase of surface roughness. Figure 12 shows the transverse and longitudinal pressure distribution at the moment of droplet impact on the soybean leaf surface. It can be seen from the figure that the pressure is mainly concentrated on the edge of the spreading of the droplet, and the surface roughness along the longitudinal direction is larger than the transverse direction. It also can be seen from the figure that the pressure along the longitudinal direction is significantly higher than the transverse direction.

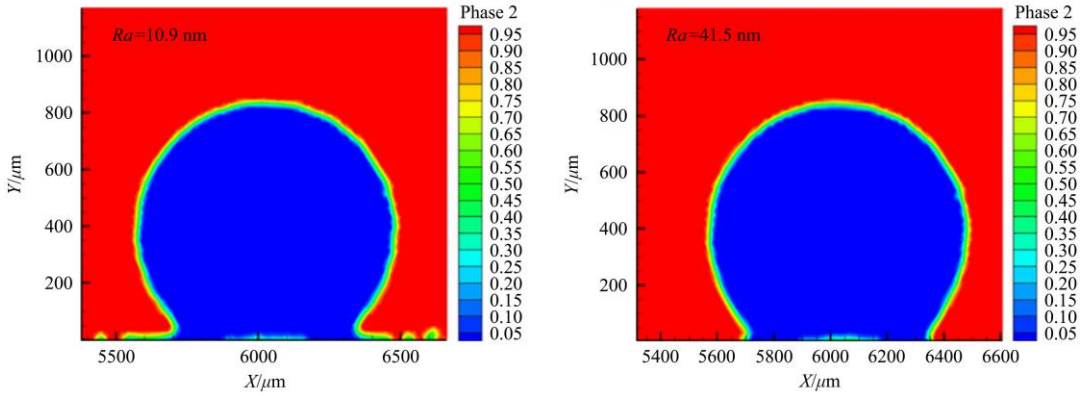

a. Transverse b. Longitudinal

Note: *Ra* is the surface roughness, nm; *X* is the wetting length of the droplet along the wall of the blade, μm; *Y* is the length of the droplet along the vertical direction, μm.

Figure 11 Instantaneous liquid phase diagram of droplet impacting the blade surface

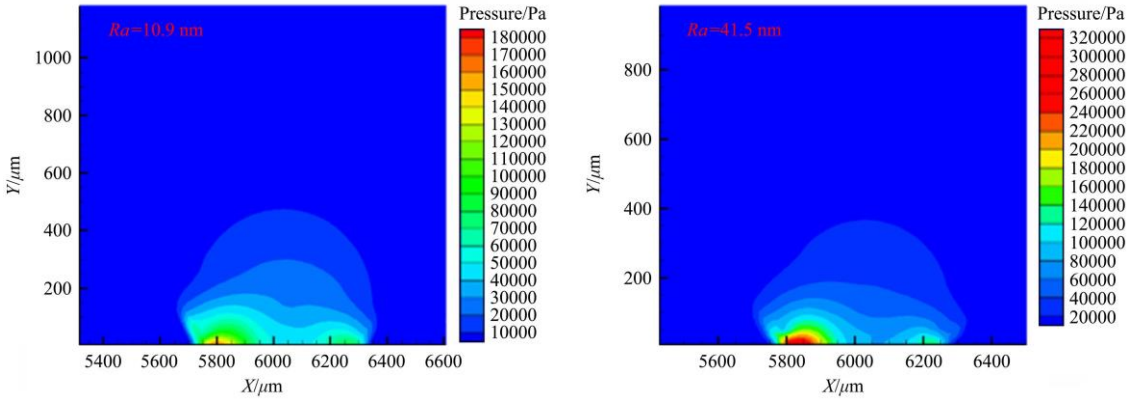

a. Transverse b. Longitudinal

Note: *Ra* is the surface roughness, nm; *X* is the wetting length of the droplet along the wall of the blade, μm; *Y* is the length of the droplet along the vertical direction, μm.

Figure 12 Instantaneous pressure distribution of droplet impacting the blade surface

3.4.3 Spreading speed

Figure 13 shows the velocity changes along the transverse (Figure 13a) and longitudinal (Figure 13b) of the droplet vertically hitting the soybean leaf surface at different impact velocities. The velocity here referred to the velocity from spreading to deposition, as shown in Figure 13. When the characteristic time t=1 ms, the value of velocity along the transverse or longitudinal direction first increases sharply, and then gradually decreases to the minimum value when t = 6 ms. Whether transverse or longitudinal, when the impact velocity is 1.34 m/s, the spreading velocity is the highest about 2.76/1.74 m/s (transverse/ longitudinal), followed by 1.55 m/s and 1.03 m/s. The maximum velocity values of the two are 2.48/1.56 m/s and 2.28/1.48 m/s, respectively.

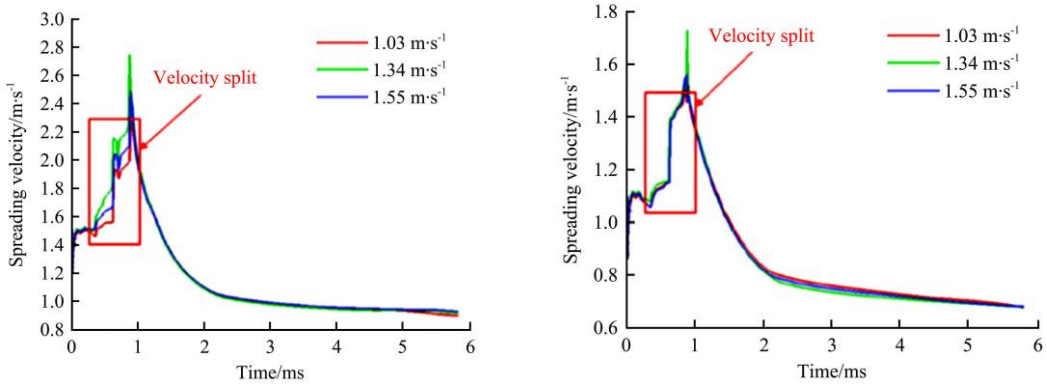

a. Transverse b. Longitudinal

Figure 13 Changes of spreading velocity of droplet impacting soybean leaf surface with time under different impact velocities

As shown in Figure 13, under the three impact velocities, the droplet velocity along the transverse direction was greater than that along the longitudinal direction when it hit the soybean leaf surface. When t=1 ms, the spreading velocity reached the maximum. The spreading velocity varies greatly within the range of 0.4-1.0 ms characteristic time (Shown in the red box in Figure 13). During this period, the vertical momentum of the droplet causes radial flow, and the kinetic energy of the droplet is partly dissipated by viscous force, partly converted into surface energy, and partly converted into radial kinetic energy during spreading. Surface energy is associated with a significant increase in the free surface area[28]. Figure 14 and Figure 15 respectively show the velocity vector distribution along the transverse and longitudinal directions when the droplet hits the soybean leaf surface at the maximum spreading

velocity. The black curve is the gas-liquid interface of the droplet, and the movement of the droplet after hitting the soybean leaf surface is basically symmetrical. As can be seen from the figures, under the action of air and wall, the velocity vector arrow at the left end of the droplet is in the left direction. Similarly, the right end of the droplet is in the right direction, so it can be seen that the droplet is in a spreading state. The transverse roughness of soybean leaf is much lower than the longitudinal roughness, the droplet transverse resistance along the leaf surface is small, and the spreading speed of droplet along the leaf surface is larger than that along with the longitudinal spreading speed. As can be seen from the figures, when the droplet hits the blade, the spreading speed along the transverse direction is obviously greater than that along the longitudinal direction.

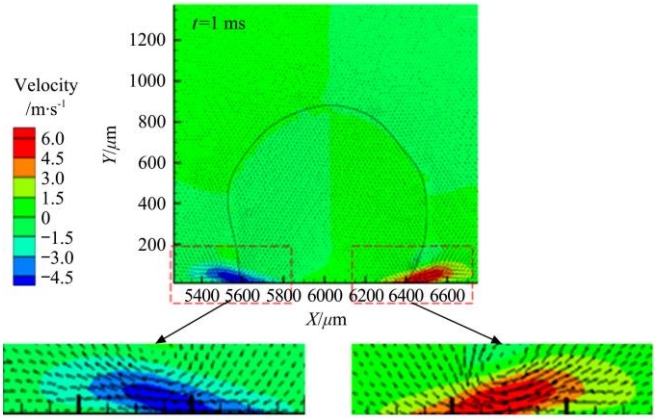

Figure 14 Velocity vector distribution of droplet impacting soybean leaf surface (transverse)

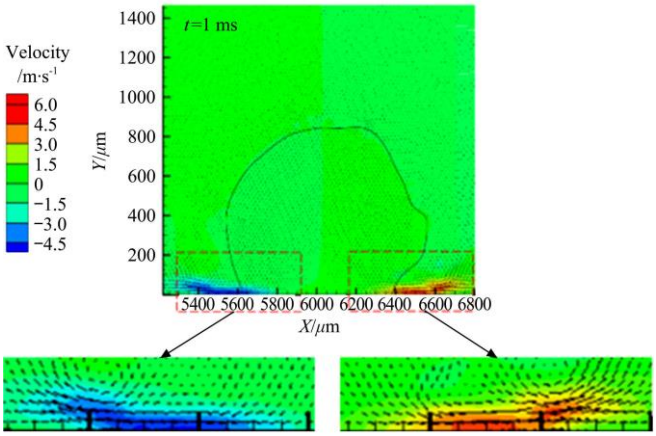

Figure 15 Velocity vector distribution of droplet impacting soybean leaf surface (longitudinal)

3.4.4 Wetting length

Let the droplet diameter be 900 μm, and the droplet impact on the soybean leaf surface was simulated and analyzed under different impact velocities. Figure 16 shows the dimensionless wetting length change over time when the droplet size was 900 μm and the droplet hit the soybean leaf at three different speeds. The ratio of the spreading length to the original droplet diameter D/D_0 is defined as the dimensionless wetting length of the droplet to complete the impact kinetic behavior on the blade surface. Diameter D can be determined by the following equation[29]:

$$\left[\frac{1}{4}(1-\cos\theta_e)+0.2\frac{W_e^{0.83}}{Re^{0.33}}\right]\left(\frac{D}{D_0}\right)^3-\left(\frac{We}{12}+1\right)\frac{D}{D_0}+\frac{2}{3}=0 \quad (25)$$

where, We is the Weber number; Re is Reynolds coefficient; θ_e is the contact angle between the droplet and the surface, (°).

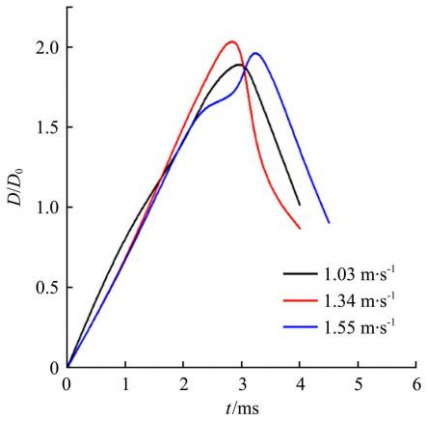

a. Transverse

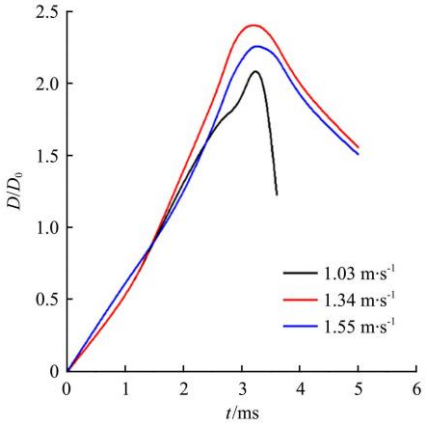

b. Longitudinal

Figure 16 Variation of the wetting length of soybean leaf impacted by droplet with time under different impact velocities

As shown in Figure 16, the entire spreading oscillation process after the droplets hit the surface of soybean leaves was mainly divided into two parts: spreading and shrinking. For all droplets, when t=0-3 ms, the droplets were in the spreading stage; when t= 3 ms, the droplets' diameter was spread to the maximum length, and the wetting length was maximum; After t=3 ms, the droplets were in the phase of contraction, the wetting length was gradually smaller, and the droplets were finally deposited on the blade. In general, the spreading and shrinking behaviors of droplets at three different speeds occurred more quickly in the transverse direction than in the longitudinal direction. For example, when the impact velocity was 1.55 m/s, the approximate spreading/shrinking time along the transverse and longitudinal directions of the blade was 3/1.1 ms (spreading/shrinking time, transverse) and 3.3/1.7 ms (spreading shrinking time, longitudinal), respectively. When the impact velocity was 1.03 m/s, the droplet shrunk more rapidly along the longitudinal side of the soybean leaf than the transverse side, and the dimensionless wetting length D/D_0 along the longitudinal side of the soybean leaf was also greater than the transverse direction. Figure 16 also shows that the wetting ability of the droplets along the transverse and longitudinal sides of the blade is consistent at three different impact velocities, reaching the maximum at 1.34 m/s, followed by 1.55 m/s and 1.03 m/s. When the impact velocity was 1.34 m/s, the droplets were more likely to spread on the soybean leaf surface.

Figure 17 shows the dimensionless wettability length change over time after droplets of four different particle sizes hit the soybean leaves at the impact velocity of 1.34 m/s. Similarly, the droplet reached its maximum wetting length at t=3 ms; when t=3-6 ms, the droplet was in the phase of contraction; After t=6 ms, the

droplets began to oscillate and eventually deposited on the blade surface. In general, the spreading and shrinking behaviors of four kinds of droplets with different particle sizes occurred almost simultaneously in the transverse and longitudinal directions. Figure 17 also shows that the wettability of droplets transversely and longitudinally along the blade was consistent at four different particle sizes, reaching its maximum at particle size equal of 985 μm, followed by 960 μm, 925 μm, and 900 μm. When the droplet size was 985 μm, the pesticide droplet was more likely to spread on the soybean leaf surface.

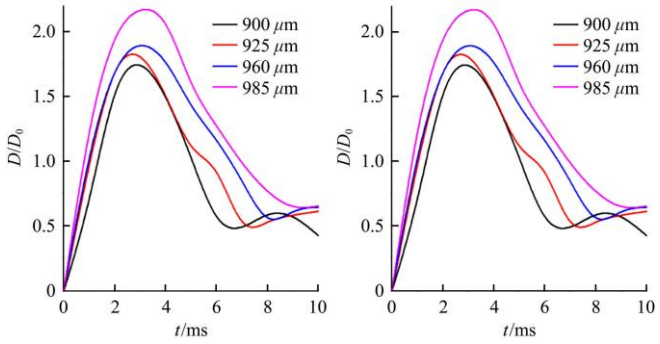

a. Transverse b. Longitudinal

Figure 17 Variation of wetting length of soybean leaf impacted by droplet with time under different particle sizes

4 Experimental verification of droplet impingement on Soybean Leaves

4.1 Experimental apparatus

The process of liquid droplets hitting soybean leaves was carried out in Bionic Intelligent Interface Science Laboratory, Technical Institute of Physics and Chemistry, Chinese Academy of Sciences. The test platform is shown in Figure 18. Using injection pump (CP-2200, Beijing, China) with matching rated capacity of 20 mL injection tube and 30 needles (0.14 mm Inner diameter, 0.32 mm outer diameter, 13 mm needle length); dual-fiber xenon high-focus light source (CEL-X250, Beijing, China), high speed camera (GC-PX100BAC, JVC, Japan) and supporting image acquisition system can clearly record the whole process of liquid droplets hitting soybean leaves at the speed of 5000 frames/s. The electronic balance (JA3003N, Shanghai, China) was used to weigh the mass of the droplet; rotating table and test bench were height adjustable. Dynamic surface tension was measured using the automatic maximum bubble pressure tensiometer (KrüssBP100, Germany), and droplet viscosity was measured using the rotary (ViscoQC^{TM}100, Anton Paar, Austria).

1. High-speed camera 2. Liftable bracket 3. Three-dimensional mobile test bench 4. Video processor 5. Xenon light source 6. Syringe pump

Figure 18 Physical diagram of the experimental device

The video of liquid droplets hitting the surface of soybean leaves was shot at 5000 frames/s, as shown in Figure 19. The test video was recorded using I-Speed Suite software and opened in I-Speed Suite software. Then, the video was played according to the number of frames (0.1 ms/frame), and the pixels before the droplets hit the surface of soybean leaves were measured. Click the Select Point in the Analyze command, pixel data on the *X*- and *Y*-axes would be generated at this time, and the left and right data on the *X*-axis of the droplet would be recorded. The pixel value after the droplet hits the surface of the soybean leaf would be measured, and the data would be recorded once for each frame. Finally, Equation (26) was used to get the maximum spreading diameter (D_{max}) of the droplet.

$$\frac{X_1 - X_2}{D_0} = \frac{X_i - X_j}{D_{max}} \tag{26}$$

where, X_1 and X_2 are the *X*-axis pixel values on the left and right sides before droplet impact; X_i and X_j are *X*-axis pixel values on the left and right sides after droplet impact; D_0 is the actual measured particle size of the droplet, mm.

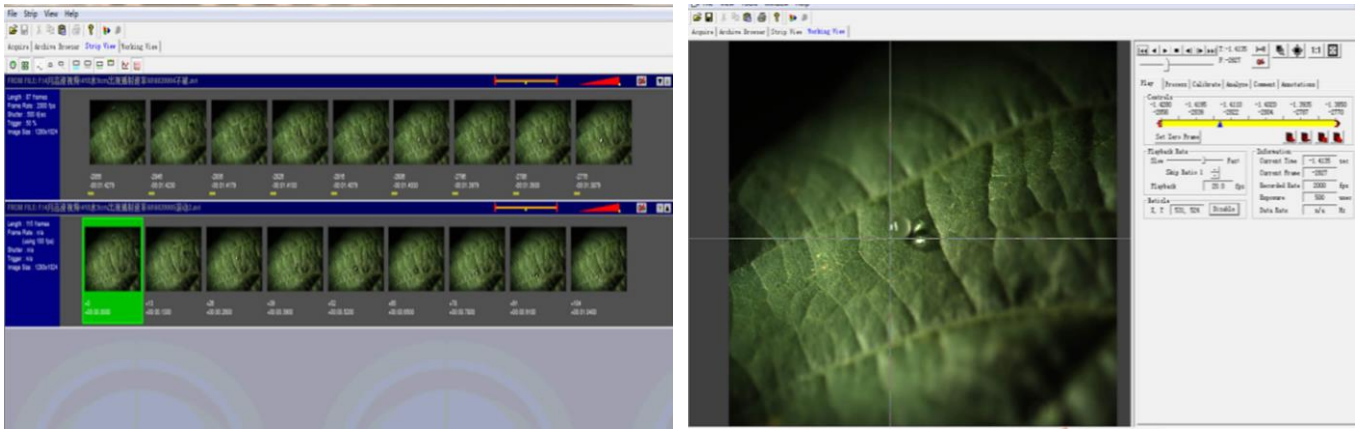

Figure 19 I-Speed suite video processing software operation interface

4.2 Influence of different impact velocities on the spreading characteristics of droplets

The droplet with a particle diameter of 900 μm was selected by the injection pump to impact the leaf surface. The droplet impact height was set to be 50 mm, 110 mm and 150 mm, and the corresponding impact velocity was 1.03 m/s, 1.34 m/s and 1.55 m/s. The whole process of droplet impact on soybean leaf was analyzed and recorded by a high-speed camera.

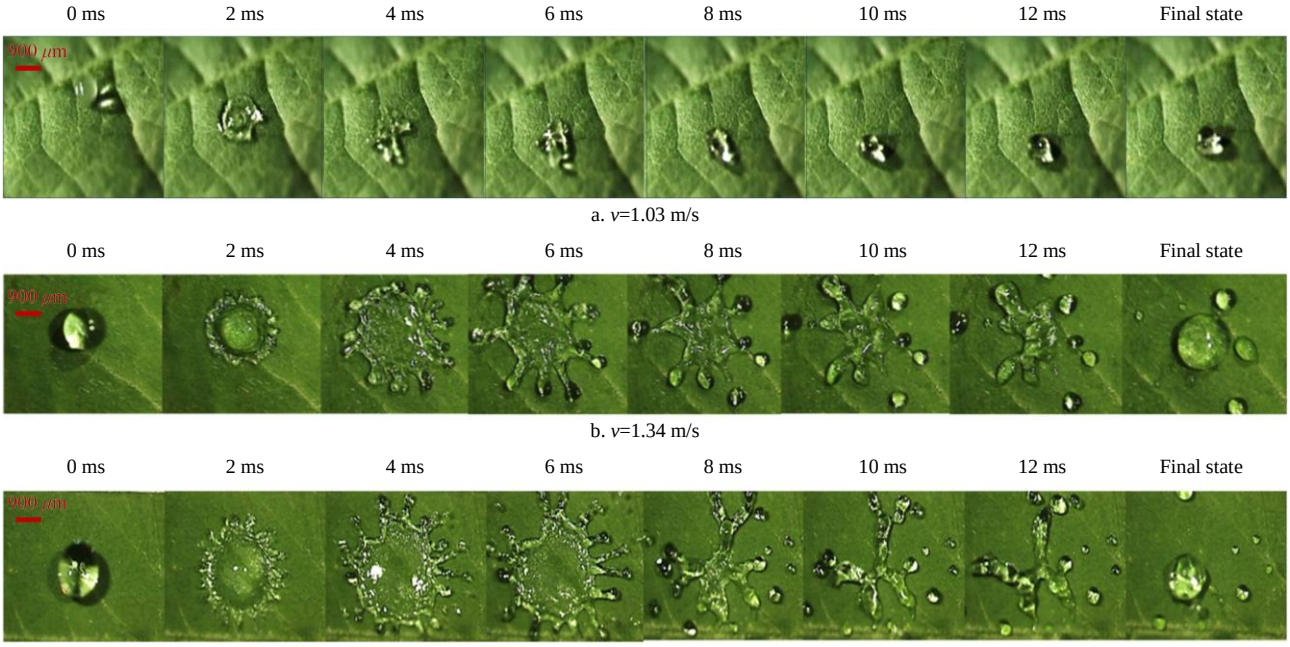

a. v=1.03 m/s

b. v=1.34 m/s

c. v=1.55 m/s

Figure 20 Droplet impacts soybean leaf surface at different impact velocities

It can be seen from Figure 20a that when the impact velocity was 1.03 m/s, the number of *We* and *Re* were 13.06 and 311.07, respectively. At 0-3 ms, the droplet impacting the blade spread to a maximum diameter of 1970 μm, and 4-10 ms was the stage of droplet withdrawal, and the droplet was deposited on the blade eventually. As can be seen from Figure 20b, when the impact velocity was 1.34 m/s, the number of *We* and *Re* were 22.11 and 404.70, respectively, and when the impact velocity was 0-3 ms, the droplet spread to a maximum diameter of 2021 m. As the impact velocity increased, the droplet impact kinetic energy increased and the droplet fragmentation phenomenon occurred. It can be seen from Figure 20c that when the impact velocity was 1.55 m/s, the number of *We* and *Re* were 29.59 and 468.12 respectively. When the impact velocity was 0-3ms, the droplet spread to a maximum diameter of 1975 m. By comparing Figures 20b and 20c, it can be seen that when the impact velocity was 1.55 m/s, the number of droplet breakage increased.

In order to deeply study the influence of impact velocity on the spreading characteristics of droplet, experiments were conducted on droplets with an impact velocity of 0.89-1.55 m/s, and Table 2 was obtained: The number of droplets broken under different impact velocities. It can be concluded from Table 2 that when the impact velocity ≥1.03 m/s, the number of droplets breaking, splashing and bouncing off the blade surface increases rapidly with the increase of impact velocity; when the number of *We*≥19.24, there are different degrees of breaking and splashing during the impact process; when *We*<19.24, there is no splashing phenomenon.

Table 2 Number of droplets broken at different impact velocities

Impact speed/m s^{-1}	Number of droplets broken	Number of drops popping
0.89	0	0
1.03	0	0
1.25	6	1
1.34	12	5
1.43	26	15
1.55	31	21

Figure 21 and Figure 22 are obtained by impact experiments on droplets with impact velocities of 0.89-1.55 m/s. Figure 21 shows the variation of the sample blade with the impact velocity of the droplet. It can be concluded that the number of the droplet is ejected by the droplet after impact crushing, and the impact velocity of the droplet is in line with the equation as follows:

$$Y = 90.651x^2 - 188.94 + 96.936 \quad (27)$$

where, Y is the number of the droplet ejected by the droplet after impact crushing; x is the impact velocity of the droplet, m/s.

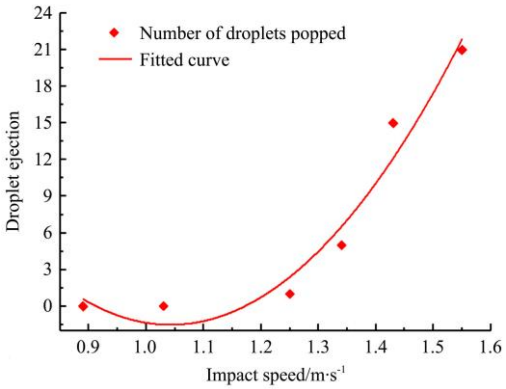

Figure 21 Liquid droplet ejection quantity and impact velocity fitting curve

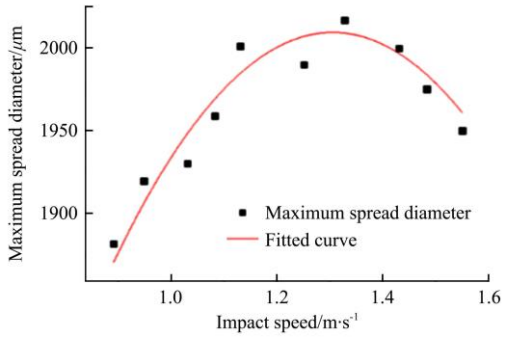

Figure 22 Fitting curve of the maximum spreading diameter of droplet and impact velocity

Figure 22 shows the variation of the maximum spreading diameter of the droplet with the impact velocity of the droplet. It can be concluded that the relationship between the maximum

spreading diameter and the impact velocity of the droplet is functional as Equation (28).

$$y = -0.8108x^2 + 2.11598x + 0.62899 \quad (28)$$

where, y is the maximum spreading diameter, μm; x is the impact velocity of the droplet, m/s.

According to Figure 21, the number of sample blades ejected by droplet crushing gradually increases with the increase of droplet impact velocity. According to Figure 22, the maximum spreading diameter of the droplet first increases and then decreases with the increase of droplet impact velocity. When the impact velocity was 1.34 m/s, the number of *We* was 22.11, and the maximum spread diameter was 2021 μm. When the impact velocity (U) was less than 1.03 m/s, the spread diameter gradually increased; when 1.03 m/s<U<1.34 m/s, the droplets began to break, splash and bounce off the leaf surface, and the spreading diameter of the droplets deposited on the leaf surface of soybean was still in the state of increase; when the impact velocity was greater than 1.34 m/s, the number of droplets breaking, splashing and bouncing off the blade surface increased sharply, and the spreading diameter of droplets decreased gradually. When the impact velocity was 1.34 m/s, the spreading characteristic of the droplet hitting the soybean leaf surface was the best.

4.3 Influence of different particle sizes on the spreading characteristics of droplets

The surface spreading characteristics of soybean leaf impinged by a single droplet were studied under different droplet sizes. Droplets of different particle sizes hitting the blade were photographed from the side, that is, the high-speed camera was parallel to the sample blade. At the impact velocity of 1.34 m/s, the video screenshots of the droplet impacting the blade with particle sizes of 925 μm, 960 μm, and 985 μm are shown in Figure 23. In Figure 23a, when the droplet diameter is 925 μm, *We* is 22.73, *Re* is 415.94. When t=0-3 ms, droplet impacting the blade spread to the maximum diameter of 2048 μm, and the maximum spreading coefficient was 2.214; When t=4-6 ms, droplet was in the withdrawal stage; When t=7-8 ms, droplet had a rebound trend after the withdrawal; When t=9-12 ms droplet popped out of the blade, and finally the droplet stopped on the sample blade. In Figure 23b, when the droplet diameter is 960 μm, *We* is 23.59, *Re* is 431.68. When t=0-3 ms, droplet impacting the blade spread to the maximum diameter of 2150 μm, and the maximum spreading coefficient was 2.240; In the withdrawal stage (t=4-7 ms), droplet tended to shrink and break into 2 droplets; When t=8-10 ms, droplets retreated into one droplet and tended to rebound; When t=11-14 ms, droplet began to rebound, and the final state of the droplet stopped on the leaf surface. In Figure 23c, when the droplet diameter is 985 μm, *We* is 24.08, *Re* is 440.67. When t=0-3 ms, droplet impacting the blade spread to the maximum diameter of 2365 μm, and the maximum spreading coefficient was 2.401; In the withdrawal stage (t= 4-7 ms), the droplet tended to be broken into 2-3 droplets. From 10 ms to the final state, the droplets were withdrawn again into one droplet on the sample blade.

To sum up, under the same impact velocity, the larger the droplet size is, the larger the droplet maximum spreading diameter is and the larger the droplet maximum spreading coefficient is. When the particle size was less than 985 μm, the droplets bounced off the blade surface; when the particle size was greater than or equal to 985 μm, it was difficult for the droplet to bounce off the sample blade due to the increase of spreading area and blade surface adhesion. The wettability was best when the droplet size was 985 μm.

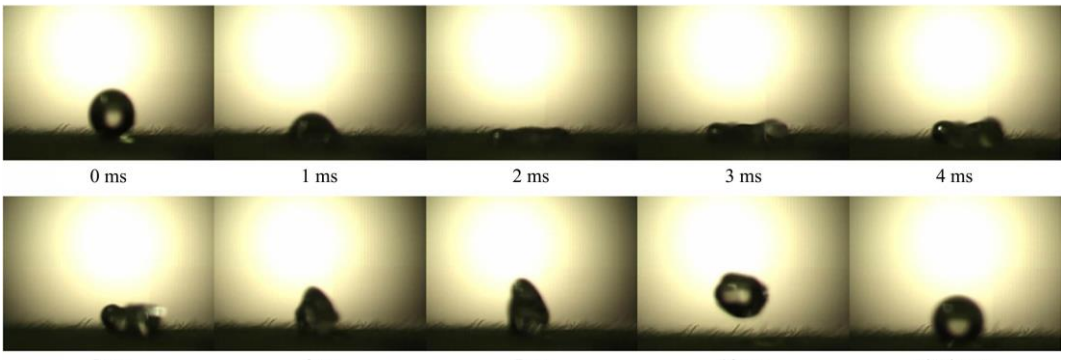

a. D_0=925 μm

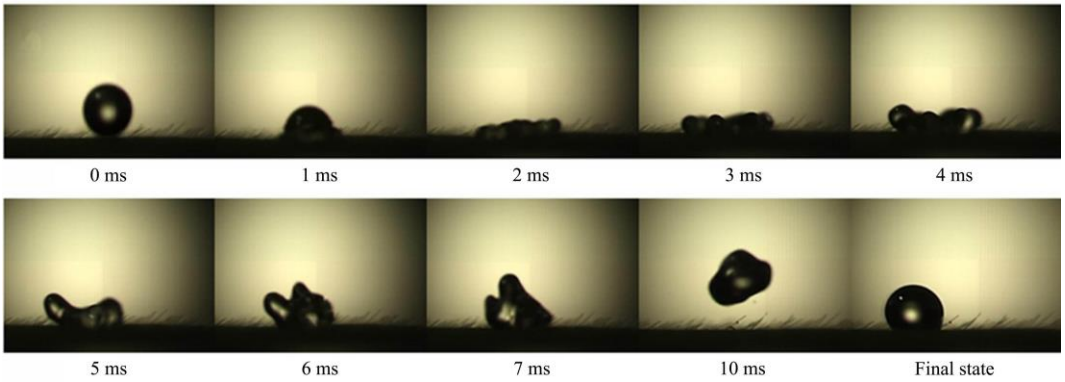

b. D_0=960 μm

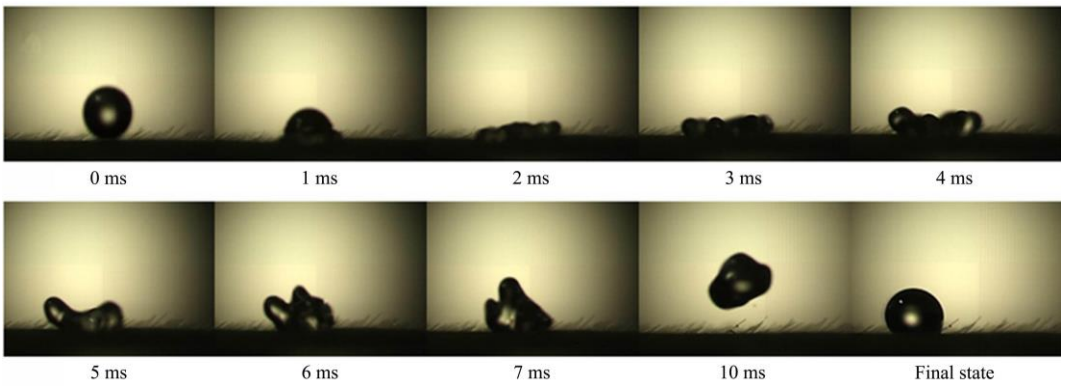

c. D_0=985 μm

Figure 23 Droplets hitting soybean leaves at the same height under different particle sizes

5 Conclusions

The kinetic and kinetic behaviors of droplets impinging on the leaf surface of soybean can determine whether pesticides can be deposited on the leaf surface effectively. In order to improve the droplet deposition efficiency, this study conducted simulation and tests on droplet impact on soybean leaf surface and drew the following conclusions:

1) Based on the actual leaf surface parameters of soybean, a two-dimensional leaf surface model was established to simulate the impact dynamics of droplets under different impact velocities and particle sizes. The effects of impact velocity and particle size on spray deposition characteristics were evaluated laterally and longitudinally from four aspects: liquid phase, surface wettability, pressure and velocity distribution, the following patterns were found: the maximum spreading diameter of the droplet first increases and then decreases with the increase of impact velocity. When the impact velocity was 1.34 m/s, the maximum spreading diameter reached its maximum value.

2) A test platform based on high-speed camera technology was constructed. 900 μm droplets were selected for the experiment to study the spreading characteristics of soybean leaf surface impacted by a single liquid drop at different impact velocities. When the impact velocity (U) was less than 1.03m/s, the spreading diameter increased gradually; When 1.03 m/s<U<1.34 m/s, the droplet began to break, splash and bounce off the leaf surface, and the spreading diameter of droplet deposited on the leaf surface of soybean was still in an increasing state; When the impact velocity (U) was greater than 1.34 m/s, the number of droplets breaking, splashing and bouncing off the blade surface increased sharply, and the spreading diameter of droplets decreased gradually. When the impact velocity was 1.34 m/s, the spreading characteristic of the droplet hitting the soybean leaf surface was the best. The surface spreading characteristics of soybean leaf impacted by a single droplet with different droplet sizes were studied. When the impact velocity was 1.34 m/s, the larger the droplet diameter was, the larger the droplet maximum spreading diameter was and the larger the droplet maximum spreading coefficient was. When the particle size was less than 985 μm, the droplets bounced off the blade surface; when the particle size was greater than or equal to 985 μm, it was difficult for the droplet to bounce off the sample blade due to the increase of spreading area and blade surface adhesion. The best spreading wettability was obtained when the droplet size was 985 μm. The experiment verifies the authenticity of the CFD simulation.

Acknowledgements

This work was financially supported by China Agriculture Research System of MOF and MARA (Grant No. CARS-04-PS25). This work was also financially supported by the Innovation and Demonstration Sub-Project of Comprehensive Utilization Mode of Agricultural Facilities in Henan Tobacco Area Based on the Increase of Tobacco Farmers' Income (Grant No. 2018410000270095).

[References]

[1] Jia W D, Zhu H P, Dong X, Xue F. Impact of spray droplet on soybean leaf surface. Transactions of the CSAM, 2013; 44(12): 87–93, 113. (in Chinese)

[2] Yang F B, Xue X Y, Cai C, Zhou Q Q, Sun Z. Atomization performance test and influence factors of aviation special centrifugal nozzle. Transactions of the CSAM, 2019; 50(9): 96–104. (in Chinese)

[3] Tian Z W, Xue X Y, Li L, Cui L F, Wang G, Li Z J. Research status and prospects of spraying technology of plant-protection unmanned aerial vehicle. Journal of Chinese Agricultural Mechanization, 2019; 1: 37–45. (in Chinese)

[4] Qin M X, Zhang X H, Tang C L. Experimental study on the droplet impact on solid surface with different roughness. Journal of Xi'an Jiaotong University, 2017; 51(9): 26–31. (in Chinese)

[5] Hilz E, Vermeer A W P. Spray drift review: The extent to which a formulation can contribute to spray drift reduction. Crop Protection, 2013; 44(20): 75–83.

[6] Wang S, Li H L, Duan H, Cui Y T, Sun H, Zhang M J, et al. Directed motion of an impinging water droplet—seesaw effect. Journal of Materials Chemistry A, 2020; 8(16): 7889–7896.

[7] Boukhalfa H H, Massinon M, Belhamra M, Lebeau F. Contribution of spray droplet pinning fragmentation to canopy retention. Crop Protection, 2014; 56: 91–97.

[8] Nairn J J, Forster W A, van Leeuwen R M. 'Universal' spray droplet adhesion model–accounting for hairy leaves. Weed Research, 2013; 53(6): 407–417.

[9] Damak M, Mahmoudi S R, Hyder N. Enhancing droplet deposition through in-situ precipitation. Nature Communications, 2016; 7(1):12560. doi: 10.1038/ncomms12560.

[10] Liang C. Numerical study on the dynamic characteristics of liquid droplets impinging on solid wall and thin liquid film. Master dissertation. Chongqing: Chongqing University, 2013; 106p. (in Chinese)

[11] Bi F F, Guo Y L, Shen S Q, Chen J X, Li C Q. Experimental study of spread characteristics of droplet impacting solid surface. Acta Physica Sinica, 2012; 61(18): 293–298. (in Chinese)

[12] Xie Y X, Mu S, Chen X M, Liu S S, Wu J, Wang H. Experiment research and simulated analysison spreading characteristics of droplet impacting wolfberry leaf. Journal of Chinese Agricultural Mechanization, 2019; 7: 70–74. (in Chinese)

[13] Wang P, Qi L J, Li H, Ji R H, Wang H. Influence of plant leaf surface structures on droplet deposition. Transactions of the CSAM, 2013; 44(10): 75–79. (in Chinese)

[14] Zheng Z W, Li D S, Qiu X Q, Zhu X L, Ma P Y, Zhang D. Numerical

analysis of effect of impacting velocity on diesel droplet impacting on inclined surface. Transactions of the CSAM, 2016; 47(8): 317–324. (in Chinese)

[15] Liang C, Wang H, Zhu X, Ding Y D, Liao Q. Numerical simulation of dynamic process of droplet impacting on different wetted surfaces. Journal of Chemical Industry and Engineering (China), 2013; 64(08): 2745–2751. (in Chinese)

[16] Liu D M, Zhou H P, Zheng J Q, Ru Y. Oblique impact behavior of spray droplets on tea tree leaves surface. Transactions of the CSAM, 2019; 50(5): 96–103, 195. (in Chinese)

[17] Li D S, Qiu X Q, Zheng Z W, Cui Y J, Ma P Y. Numerical analysis of droplet impact on surfaces with different wettabilities. Transactions of the CSAM, 2015; 46(7): 294–302. (in Chinese)

[18] Zhao H, Song J L, Zeng A J, He X K. Relationship between dynamic surface tension and droplet diameter. Transactions of the CSAM, 2009; 40(8): 74–79. (in Chinese)

[19] Ding L, Yang L, Zhang D X, Cui T, Gao X J. Optimization design and experiment of corn air suction seed metering device seed plate based on DEM-CFD coupling method. Transactions of the CSAM, 2019; 50(5): 50–60. (in Chinese)

[20] Ding L, Yang L, Wu D H, Li D Y, Zhang D X, Liu S R. Simulation and experiment of corn air suction seed metering device based on DEM-CFD coupling method. Transactions of the CSAM, 2018; 49(11): 48–57. (in Chinese)

[21] Song Y C, Wang C H, Ning Z. Computation of incompressible two-phase flows by using CLSVOF method. Transactions of the CSAM, 2011; 42(7): 26–31, 60. (in Chinese)

[22] Zhang H. Droplet Impact Dynamics on Randomly Rough Surfaces: A Computational Study. Master dissertation. Suzhou: Suzhou University, 2015; 65p. (in Chinese)

[23] Liu Y H, Andrew M, Li J, Yeomans J M. Symmetry-breaking in drop bouncing on curved surfaces. Nature Communications, 2015; 6(1): 10034. doi: 10.1038/ncomms10034.

[24] Li X Y. Experimental and theoretical studies of water droplet impacting dry solid surfaces. Doctoral dissertation. Dalian: Dalian University of Technology, 2010; 125p. (in Chinese)

[25] Dong X. Systematic investigation of 3-dimentional spray droplet impaction on leaf surfaces. Doctoral dissertation. China Academy of Agricultural Mechanization Sciences, 2013; 132p. (in Chinese)

[26] Pan Z Z. Study on the preparation of Lambda-cyhalothrin Nanosuspension. Master dissertation. Changchun: Jilin University, 2015; 78p. (in Chinese)

[27] Cui Y T, Qin C B, Zhang Z, Liu D Q, Dong H F, Zhang K F, et al. Experimental study on the impact of droplets on the surface of soybean leaves. Soybean Science, 2018; 37(6): 961–968. (in Chinese)

[28] Gil E, Balsari P, Gallart M, Llorens J, Marucco P, Andersen P G, et al. Determination of drift potential of different flat fan nozzles on a boom sprayer using a test bench. Crop Protection, 2014; 56: 58–68.

[29] Versteeg H K, Malalasekera W. An introduction to computational fluid dynamic: The finite volume method. New York: Wiley, 1995; 257p.